DC Servomotor-based Antenna Positioning Control System Design using PID and LQR Controller

Linus A. Alwal, Peter K. Kihato and Stanley I. Kamau

Abstract— There are increasing needs to develop control systems that can be used to automatically point Direct Current (DC) servomotor driven parabolic antennas to moving targets, notably in satellite tracking, to maintain the desired line of sight for quality communication. Although many researchers nowadays focus on artificial intelligence (AI) techniques, this work reckons that a well designed optimal linear controller can still give acceptable results at reduced system cost and complexity.

In this paper the design and control of DC servomotor-based antenna positioning system has been addressed and simulated in MATLAB/SIMULINK software. The response of the system is analyzed and results are first obtained by using well tuned Proportional-Integral-Derivative (PID) controller. The PID controller is then replaced by Linear Quadratic Regulator (LQR) which apart from optimizing the system response increases the accuracy of the state variables by estimating the states. It has been shown that the LQR results are much better than the results obtained by PID controller in terms of reduced steady state error, settling time and overshoot. Moreover, since low speed rotations are required and assuming linear conditions, the results obtained with LQR method can challenge those obtained by AI based techniques

Keywords— Antenna-Positioning Systems, DC servomotor, Linear Quadratic Regulator-LQR, PID Controller

I. INTRODUCTION

Parabolic antennas mounted at earth stations which are commonly used in satellite tracking applications, are susceptible to suffer from environmental disturbances [1]. For many years, DC servomotor-based controllers have been in use to automatically position the satellite dishes [2]. Several controller models have been developed over time to solve the problem of antenna pointing in satellite and movable targets tracking using servomechanism [3], [4] and [5]. The case of overseas satellite telecommunication is considered in [3] where the control system directs on-board motorized antenna towards a selected satellite. Fault Tolerant Control (FTC) system is designed using the ship simulator facility to maintain the tracking functionality. However, the fault estimation has proved to be an extremely challenging task. An overview of most common servomotor-based linear antenna pointing mechanisms: Proportional-Integral (PI), Proportional-Integral-Derivative (PID), Linear Quadratic Gaussian (LQG) modeled and implemented for varied space applications is provided in [5]. PI controllers are easy to implement but take much time to reach setpoint and have degraded performance under system nonlinearities. LQG controllers are not only optimal but also have the ability to estimate non-measurable states by using observers to reconstruct them and provide better performance in case of wind gusts noise. However, the performances of these methods depend on the accuracy of system models and parameters. Generally, an accurate non-linear model of actual DC motor is difficult to find. Recently, new intelligent control techniques such as Neural Networks, Genetic Algorithms, Fuzzy Logic and hybrid AI methods are under research consideration as a viable solution to the problem [5]. The DC servomotor suitable for automatic dish antenna positioning in the case system ought to possess a minimum torque of 5.0Kg.cm at low speed and a maximum torque of 7.9Kg.cm at full speed. Within those ranges, the motor can support the following categories of dish antenna sizes: 0.30m, 0.45m, 0.55m and 0.60m nominal diameter, weighing from 4Kg to 7.0Kg for typical material and design.

A. Problem Formulation

The objective is to design PID and LQR controller for the system under study to meet the following tracking specifications: rise time $(t_r) \le 4s$, settling time $(t_s) \le 5s$ and overshoot $(M_p \le 10\%)$. These performance requirements conform to the standards of a practical industrial system.

B. System Description

Fig.1 is the control block diagram of the DC servomotor antenna pointing system [6]. The first input to the summer is set position $r(t)$, the desired position at which the azimuth or elevation motor is expected to run to.

Linus A. Alwal, Department of Electrical and Electronic Engineering, JKUAT, (phone: +254729747653; e-mail: laloo@jkuat.ac.ke);
Peter K. Kihato, Department of Electrical and Electronic Engineering, JKUAT, (e-mail: pkihato@jkuat.ac.ke);
Stanley .I. Kamau, Department of Electrical and Electronic Engineering, JKUAT, (e-mail: skamau@eng.jkuat.ac.ke).

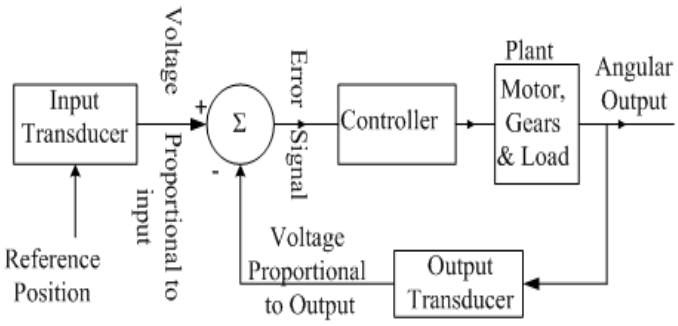

Fig.1 Block diagram of antenna control mechanism

The second input is the feedback signal, the current position of the respective motor, captured by some feedback sensor like the potentiometer and changed to a summer readable format. The difference between these two inputs, called position error signal $e(t)$, is given to the controller that reads the error signal and produces appropriate output signal, controller output $u(t)$.The controller output then reaches the motor driver, which produces a proportional output to rotate the respective motor in either direction according to the sign of the error signal. As the desired position is approached, the error signal reduces to zero and the motor stops [7].

C. *Mathematical Modeling of DC Servomotor System*

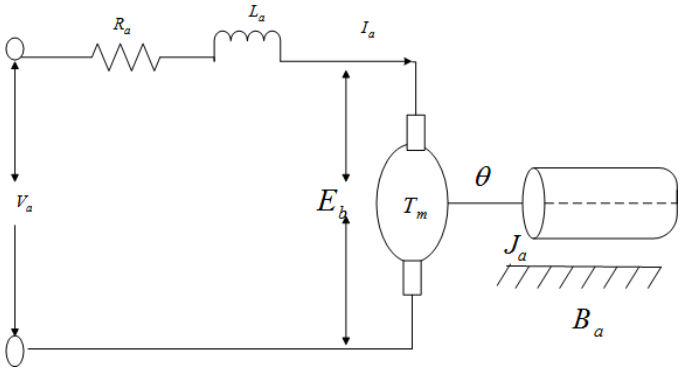

Fig.2 DC motor circuit diagram

Fig. 2 represents the DC (servo) motor model [6], [7]. Reference is made to the parameters defined in Table I. For an armature-controlled separately excited DC motor, the voltage applied to the armature of the motor is varied without changing the voltage applied to the field. Using Kirchoff's Voltage Law, the input armature voltage $V_a(t)$ and motor torque $T_m(t)$ is related to (1):

$$V_a(t) = R_a I_a(t) + L_a \frac{dI_a(t)}{dt} + E_b(t) \quad (1)$$

The motor torque $T_m(t)$ is related to the armature current $I_a(t)$ by a constant factor K_T given in (2):

$$T_m(t) = K_T I_a(t) \quad (2)$$

Also, the back electromotive force (e.m.f) $E_b(t)$ is related to the angular velocity by (3):

$$E_b(t) = K_T \omega_m(t) = K_T \frac{d\theta}{dt} \quad (3)$$

By Newton's and Kirchhoff's Laws, obtain (4) and (5):

$$J_a \frac{d^2\theta}{dt^2} + B_a \frac{d\theta}{dt} = K_T I_a(t) \quad (4)$$

$$L_a \frac{dI_a(t)}{dt} + R_a I_a(t) = V_a(t) - K_T \frac{d\theta}{dt} \quad (5)$$

Applying Laplace transform to (4) and (5) assuming zero initial conditions we get (6) and (7):

$$J_a s^2 \theta(s) + B_a s \theta(s) = K_T I_a(s) \quad (6)$$

$$L_a s I_a(s) + R_a I_a(s) = V_a(s) - K_T s\theta(s) \quad (7)$$

Making current the subject in (7) and substituting in (6), we get (8):

$$J_a s^2 \theta(s) + B_a s \theta(s) = K_T \frac{V_a(s) - K_T s\theta(s)}{R_a + L_a s} \quad (8)$$

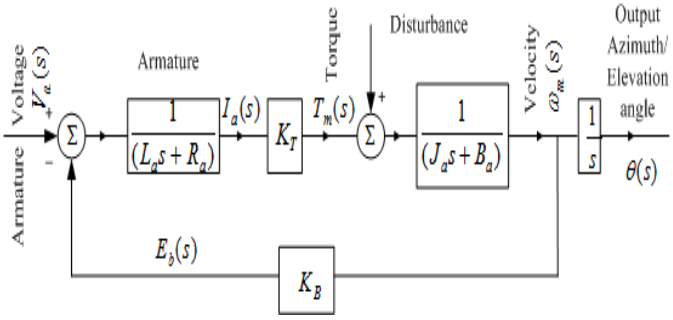

Fig.3 Block diagram of separately excited DC servomotor

Fig. 3 is a block diagram of DC servomotor system showing elements of the transfer function. From (8), the transfer function from the input voltage, $V_a(s)$ to the output angle θ directly follows (9) and to the angular velocity, $\omega_m(s)$ is (10):

$$G_a(s) = \frac{\theta(s)}{V_a(s)} = \frac{K_T}{s[(R_a + L_a s)(J_m s + B_m) + K_T K_B]} \quad (9)$$

$$G_a(s) = \frac{\omega_m(s)}{V_a(s)} = \frac{K_T}{[(R_a + L_a s)(J_m s + B_m) + K_T K_B]} \quad (10)$$

State-space form of the equations above can be expressed by selecting the rotating speed and electrical current as state variables and the voltage as an input. The output is chosen to be the rotating speed. The Linear-Time-Invariant (LTI) system is given generally as in (11):

$$\begin{cases} \dot{x}(t) = Ax(t) + Bu(t) \\ y(t) = Cx(t) + Du(t) \end{cases} \quad (11)$$

where A is an *nxn* state matrix, B is an *nxr* input matrix, C is *mxn* output matrix, D is an *mxr* matrix, $x(t)$ is an n-state vector and u(t) is r-control vector [8]. Equation (12) &

(13) gives the state-space representation of DC motor speed control:

$$\begin{bmatrix} \frac{di_a}{dt} \\ \frac{d\omega_r}{dt} \end{bmatrix} = \begin{bmatrix} -\frac{R}{L} & -\frac{K_B}{L} \\ \frac{K_m}{J} & -\frac{B}{J} \end{bmatrix} \begin{bmatrix} i_a \\ \omega_r \end{bmatrix} + \begin{bmatrix} \frac{1}{L} \\ 0 \end{bmatrix} V_a \quad (12)$$

$$y = [01] \begin{bmatrix} i_a \\ \omega_r \end{bmatrix} + [0] V_a \quad (13)$$

Using values from Table I in (12) & (13) and comparing with (11) gives (14):

$$A = \begin{bmatrix} -17.78 & -1.111 \\ 25 & -0.5 \end{bmatrix} \quad B = \begin{bmatrix} 2.22 \\ 0 \end{bmatrix},$$
$$C = [0\ 1] \text{ and } D = [0] \quad (14)$$

II. PROPORTIONAL-INTEGRAL-DERIVATIVE (PID) CONTROLLER

PID controllers are implemented in most industrial processes. This is because they are low cost, can usually provide good closed-loop response characteristics, tuned using relatively simple rules and are relatively easy to construct. Control signal is the sum of three components: proportional, integral and derivative gain scaling factors [9]. The structure of PID controller is shown in fig.4. To derive the closed-loop system transfer function without the (PID) compensator, the following assumptions were made [4]:

- The transfer functions for power amplifier and preamplifier are accurate and that saturation is never reached.
- No disturbances in the signals sent between system parts.

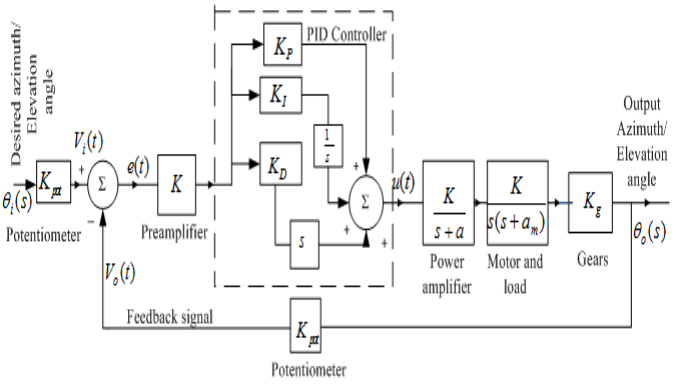

Fig.4 Block diagram of Antenna Azimuth PID controller.

From (9), we get (15):

$$V_a(s) = \frac{[(J_m s^2 + B_m s)(R_a + L_a s) + K_T K_B s]}{K_T} \theta_m(s) \quad (15)$$

In a fixed field motor it is assumed that $K_T = K_B$.Assuming that $R_a >> L_a$ (15) simplifies to (16):

$$\frac{\theta_m(s)}{V_a(s)} = \frac{\frac{K_T}{JR_a}}{s(s + \frac{B_m R_a + K_T K_B}{JR_a})} \quad (16)$$

The system parameters including the DC servomotor are given in Table I [4], [6]. Using the gear ratio, the transfer function relating load displacement to motor armature voltage is (17):

$$\frac{\theta_o(s)}{V_a(s)} = 0.1 \frac{K_m}{s(s + a_m)} = \frac{0.2083}{s(s + 1.71)} \quad (17)$$

The open-loop transfer function for output angular velocity $\omega_o(t)$ without feedback [5] is given in (18):

$$G_a(s) = \frac{\omega_o(s)}{V_p(s)} = \frac{20.83}{s^2 + 101.71s + 171} \quad (18)$$

The closed-loop transfer function without the PID compensator [11] is found by using (18) and the block diagram reduction [9] to get (19):

$$\frac{\theta_o(s)}{\theta_i(s)} = \frac{6.63K}{s^3 + 101.71s^2 + 171s + 6.63K} \quad (19)$$

TABLE I
PARAMETERS OF MODEL WITH DC SERVOMOTOR

SCHEMATIC PARAMETERS		
PARAMETER	DEFINITION	AZIMUTH/ ELEVATION
a	Power Amplifier Pole	100
B_a	Motor Dampening Constant[Nms/rad]	0.01
B_L	Load Dampening Constant[Nms/rad]	1
B_m	Equivalent viscous friction coeff.[Nms/rad]	0.02
J_a	Motor Inertial Constant[Kgm^2]	0.02
J_L	Load Inertial Constant[Kgm^2]	1
J_m	Equivalent moment of inertia[Kgm2]	0.03
K_1	Power Amplifier Gain	100
K_B	Back emf Constant[Vs/rad]	0.5
K_T	Motor Torque Constant[Nm/A]	0.5
L_a	Motor Armature Inductance[H]	0.45
N	Turns on Potentiometer	10
N_1	Gear Teeth	25
N_2	Gear Teeth	250
N_3	Gear Teeth	250
Ra	Motor Armature Resistance[Ω]	8
V	Voltage across Potentiometer[V]	10
BLOCK DIAGRAM PARAMETERS		
a	Power Amplifier Pole	100
a_m	Motor and Load Pole	1.71
K	Preamplifier Gain	_
K_1	Power Amplifier Gain	100
K_g	Gear Ratio	0.1
K_m	Motor and Load Gain	2.083
K_{pot}	Potentiometer Gain	0.318

According to Routh-Herwitz criterion [6], [7], the system will give stable response with the value of K in the range 0 < K < 2623. Here, the gain value taken is 100 which had been chosen to be equal to that of the power amplifier for design convenience and to reduce energy consumption while still falling within the stability range [9]. Equation (19) becomes (20):

$$\frac{\theta_o(s)}{\theta_i(s)} = \frac{663}{s^3 + 101.71s^2 + 171s + 663} \quad (20)$$

State-space of closed-loop transfer function of antenna azimuth position control is represented as in (21):

$$A = \begin{bmatrix} -101.7100 & -171.0000 & -663.0000 \\ 1.0000 & 0 & 0 \\ 0 & 1 & 0 \end{bmatrix}$$

$$B = \begin{bmatrix} 1 \\ 0 \\ 0 \end{bmatrix}, \; C = \begin{bmatrix} 0 & 0 & 663 \end{bmatrix} \text{ and } D = \begin{bmatrix} 0 \end{bmatrix} \quad (21)$$

The PID controller in parallel form [10] is (22):

$$U(t) = K_p e(t) + K_I \int e(t) + K_D \frac{de(t)}{dt} \quad (22)$$

where K_p, K_I and K_D are proportional, integral and derivative gains and $e(t)$ = error. The transfer function of PID controller in frequency domain is represented in (23):

$$\frac{U(s)}{E(s)} = K_P + \frac{K_I}{s} + K_D s \quad (23)$$

Using PID, closed-loop transfer function, [9] is (24):

$$\frac{\theta_o(s)}{\theta_i(s)} = \frac{663K_D s^2 + 663K_P s + 663K_I}{s^4 + 1017s^3 + (171 + 663K_D)s^2 + 663K_P s + 663K_I} \quad (24)$$

The values of proportional (K_P), integral (K_I) and derivative (K_D) gains are obtained using Ziegler-Nichols tuning algorithm. This method gives automatic oscillation of the process to compute the three gain constants. Ziegler-Nichols presented two methods: Step response method and Frequency response method [10]. In this paper, frequency response method was used to obtain the preliminary gain values of the PID controller as follows: $K_P = 15$, $K_D = 90$ and $K_I = 0.625$. However, since these initial gain constants depicted high overshoots, the final PID controller gain parameters which gave the most appropriate response and thus meeting the design constraints were obtained as follows: $K_p = 18$, $K_I = 4$ and $K_D = 2$.

III. LINEAR QUADRATIC REGULATOR (LQR) CONTROLLER DESIGN

Linear Quadratic Regulator (LQR) design technique is used in modern optimal control theory and has been widely used in many control applications besides PID because of its stability [11]. It uses state-space approach to analyze and control an LTI system whose general model was represented in (11). To start LQR design the following assumptions are made:

1. Plant model defined by (11) is perfectly known.
2. All states are directly measurable (available for feedback).

If assumption 1 is not true (the model has uncertainties), robust control is preferred. If assumption 2 is not true (only the output is measurable), then an observer is required, in which case, the system must be observable. The LQR method is used to achieve acceptable system performance by minimizing the performance index (cost) value J, [12], defined for $t_f = \infty$ (steady-state case) by (25):

$$J = \frac{1}{2}\int_{t_0}^{\infty} (x^T(t)Qx(t) + u^T(t)Ru(t))dt \quad (25)$$

where $R = R^T > 0$, is weighting factor of control variables (positive definite matrix) and $Q = Q^T \geq 0$ is weighting factor of states (positive semi-definite matrix). The LQR control technique involves choosing a control law $u(t) = -Kx(t)$ in which $K = R^{-1}B^T P$ is the LQR state feedback control gain which is used to stabilize the origin (i.e. regulating x to zero). P is the unique, positive semi-definite solution of the algebraic Riccati equation (ARE) given by (26) [11], [12].

$$A^T P(t) + P(t)A + Q - P(t)BR^{-1}B^T P(t) = 0 \quad (26)$$

For $t_f = \infty$, $P(t) = P$ (constant).

Fig.5 shows block diagram of Linear Quadratic Controller for DC servomotor system.

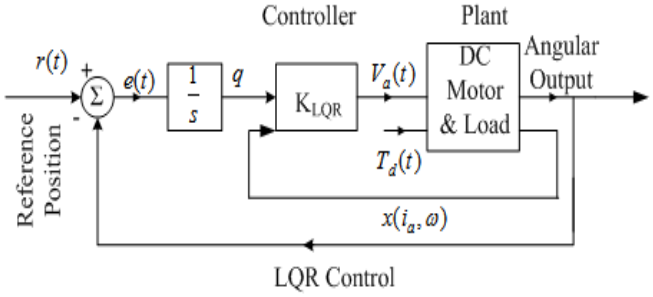

Fig. 5 Linear Quadratic Regulator control system

To design LQR controller, the first step is to select the weighting matrices Q and R. The value R weight inputs more than the states while the value of Q weight the states more than the inputs [13]. Next, the constant feedback gain vector K is computed using MATLAB 'lqr' command included in a complete code written knowing A, B, Q and R and the closed-loop system step responses is found by simulation. It is necessary to achieve proper choice of the two parameters, R and Q, to balance the relative importance of the control effort (u) and error respectively, in the cost function. In order to improve the design and tune the response, various Q matrices and R values were tried. For instance, Q matrices, [1 0; 0 10] and [1 0; 100] were used and for R, 0.1 and 0.01 were applied. It was found that increasing

the (1, 1) and (2, 2) elements of the Q matrix made the settling and rise times to go down, and lowered the angle the motor moved. In addition, it was noted that if we increased the values of the elements of Q even higher, we could improve the response even more by reducing the tracking error but this would require greater control effort u which corresponds to greater cost. The value of K that gave the desired optimized performance with respect was finally obtained as $K = [-0.65 \quad 169.0 \quad 7.1]$, which satisfied the transient design requirements.

IV. SIMULINK MODEL

The SIMULINK model for the designed PID and LQR controller system created in MATLAB software for conducting the simulations is shown in fig.6. The controller is taken as a PID controller in one case and as LQR in the other. A step input signal was taken as the reference and applied to the plant transfer function and state-space system.

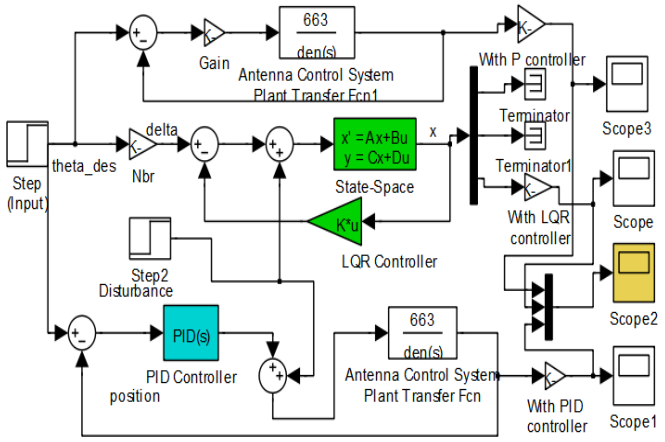

Fig.6 PID & LQR Control Simulink model layout

V. RESULTS AND DISCUSSIONS

The proposed LQR control system has been addressed through design and simulation. Further, it has been compared with the PID controller in order to evaluate its performance. Response of closed-loop antenna position control system with unity gain proportional (P) controller is shown in fig.7 from which it is noticed that the response is not good due to very high overshoot (50%). In fig. 8, the step response of the system has been improved with inclusion of PID controller which significantly reduces the value of steady-state error, the rise time and the settling time. Fig. 9 shows the system response by using LQR Controller. Fig. 10 shows on the same axes, the comparison of the system step response without any controller and with the PID and LQR controllers.

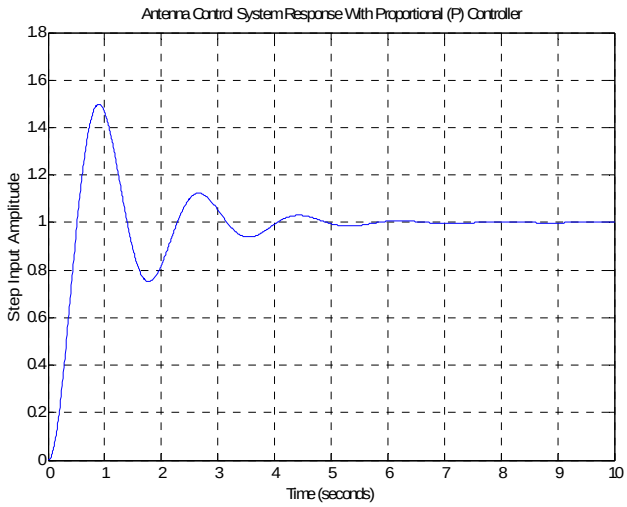

Fig.7 Step response of system with Proportional (P) controller

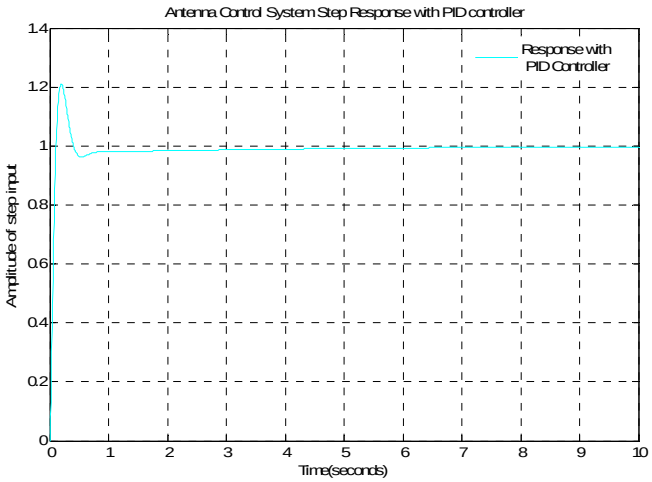

Fig.8 Step response of system with PID controller

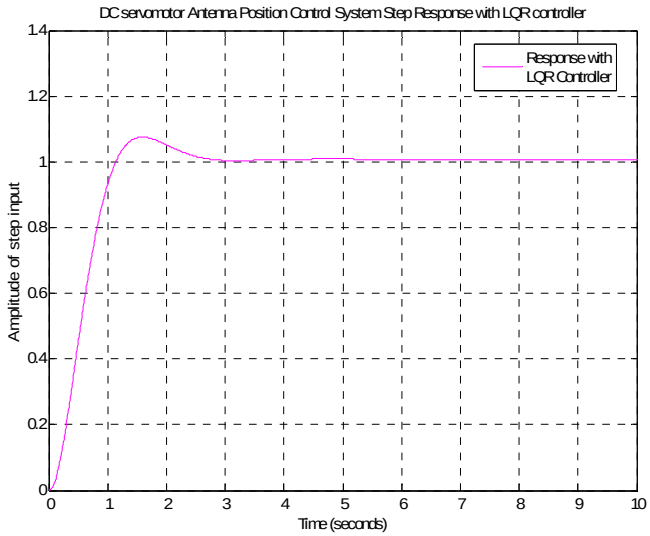

Fig.9 Antenna control system step response using LQR controller

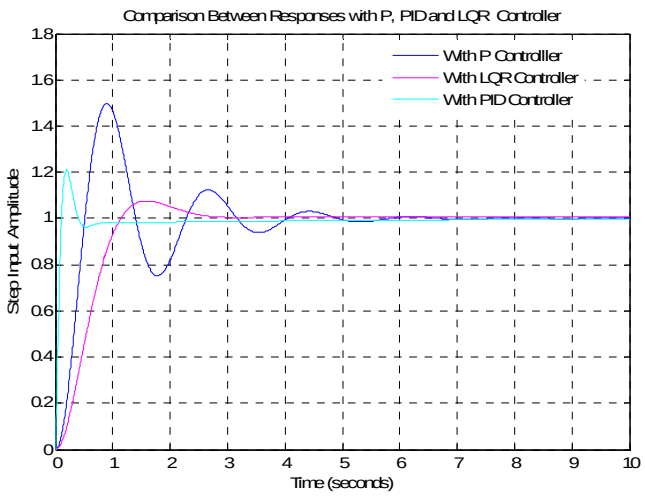

Fig.10 Step Response with P, PID and LQR Controller

From the simulation results it is seen that LQR provides response with faster settling times and reduced overshoots when compared to PID controller. The maximum overshoot with LQR is minimized to less than 4.0% while it was 20.0% with PID. The rise time is $0.4\,\text{sec}$. for PID controller and $0.9\,\text{sec}$. for the LQR for response to transit from 10.0% to 90.0% of the steady state value. It can be understood from the above summary therefore, that the LQR shows a better tracking response than the PID controller even as the reference position is changed.

VI. Conclusion and Future Work

An LQR for a DC servomotor based antenna pointing system has been designed and the performance was evaluated by simulation. The LQR satisfied all the design requirements and results indicated significant improvement in maintaining tracking of approximate zero overshoot and minimum stabilizing time as compared to the classical PID controller. The latter despite having lower rise time, suffered a lot in terms of registering higher overshoots and settling times especially in the presence of disturbance. The objectives were met in both design and software simulations. Future work is to use hybrid neuro-fuzzy based techniques optimized with nature-inspired training strategies such as particle swarm organization (PSO) and genetic algorithm (GA) and investigate on whether better results could be achieved.

References

[35] J.K. Kim, K.R. Cho and C. S. Jang, “Fuzzy control of data link antenna control system for moving vehicles," ICCAS, June 2005.
[36] T.V. Hoi, N. T. Xuan and B. G. Duong, “Satellite tracking control system using Fuzzy-PID controller," VNU Journal of Science, Mathematics and Physics, vol. 31, no. 1, pp. 36-46, 2015.
[37] M. N. Soltani, R .Zamanabadi and R. Wisniewski, “Reliable control of ship-mounted satellite tracking antenna," IEEE Transactions on Control Systems Technology, p. 99, 2010.
[38] L. Xuan, J. Estrada and J. Di Giacomandrea, “Antenna azimuth position control system analysis and controller implementation," Design Problem, July 2009.
[39] M. Ahmed, S.B. Mohd Noor, M. K. Hassan and A. B. Che Soh, “A Review of Strategies for Parabolic Antenna Control," Australian Journal of Basic and Applied Sciences, vol. 8(7), pp. 135-148, May 2014
[40] N.S. Nise, “Control System Engineering," John Wiley & Sons, 6th Edition, 2011.
[41] K. Ogata, “Modern Control Engineering," Prentice-Hall Inc. USA, 4th Edition, p.95, 2010.
[42] W.U. Orji, M. C. Christian, C. I. Egbunonu, C. K. Okorie, “Performance Analysis of Linear Quadratic Regulator Controller Design Techniques for Optimal Servomotor Speed Control” International Journal of Scientific & Engineering Research, Volume 6, Issue 4, April-2015.
[43] A.R. Chishti, S.F. Bukhari, H.S. Khaliq, M.H. Khan and S.Z. Bukhari, “Radio Telescope Antenna Azimuth Position Control System Design and Analysis in MAT LAB/Simulink using PID&LQR Controller," The Islamia University of Bahawalpur, Pakistan, 2014.
[44] P.R. Kumar and V.N Babu, “Position Control of Servo Systems using PID Controller Tuning with Soft Computing Optimization Techniques," International Journal of Engineering Research & Technology (IJERT), vol. 3, pp. 976-980, November 2014.
[45] L. Frank, L. D. Vrabie and V. L. Syrmos, “Optimal Control,” 3rd Edition’, New Jersey, USA, John Wiley and Sons, 2012.
[46] G.R. Yu and R.-C. Hwang, “Optimal PID speed control of brushless DC motors using LQR approach,” In Proc. IEEE International Conference on Man and Cybernetics, pages 473–478, Hague, Netherlands, 2004.
[47] R. S. Burns, “Advanced Control Engineering,” Butterworth Heinemann, Jordan Hill, Oxford, ISBN 0750651008, pg 274-285, 2001.